

Model for the Glauber-type calculations of beam fragmentation at low energies*

A. N. Ismailova^{†1,2,3}, Yu. L. Parfenova¹, P. G. Sharov^{1,4}, and D. M. Janseitov^{1,2}

¹Flerov Laboratory of Nuclear Reactions, JINR, 20 Joliot Curie Str, Dubna, Russia

²Institute of Nuclear Physics, 1 Ibragimov Str, Almaty, Kazakhstan

³Al-Farabi Kazakh National University, Almaty, Kazakhstan

⁴Institute of Physics, Silesian University Opava, Czech Republic

Abstract

In the present paper momentum distributions of nuclei produced in the heavy ion beam fragmentation at the relatively low energies (below 100 $A\cdot\text{MeV}$) are studied. For this study, a new theoretical approach is developed on the basis of the Glauber model [1] modified for taking into account the energy and momentum conservation laws. In this approach, the longitudinal momentum of the most neutron rich nuclei, ^{10}Be , ^9Li , ^8He , produced in a few neutron removal reactions in the ^{11}B fragmentation in the Be target at a beam energy of 35 $A\cdot\text{MeV}$ are calculated. The region of applicability of the new approach is discussed. This approach gives the asymmetric longitudinal momentum distributions at low energies, and the asymmetry is defined by the kinematical locus and geometry of the reaction (central or peripheral reactions). We analyze the changes of the phase volume and the longitudinal momentum distributions with the beam energy and number of the removed nucleons. The results of the calculations are compared to the parametrizations (see [2]) widely used for estimates of nuclear production in fragmentation for planning of nuclear experiments.

Keywords: fragmentation, Glauber model, momentum distribution, low energy nuclear reactions, neutron-rich nuclei

*This work has been supported by the Science Committee of the Ministry of Science and Higher Education of the Republic of Kazakhstan (AP19678586)

[†]Email: ismailova@jinr.ru

1 Introduction

In-flight method of the ion beam production is widely used in experimental nuclear studies. For effective functioning of the fragment separator knowledge of the longitudinal momentum distributions of fragments is of importance, especially for facilities working at low energies ($E < 100 A\cdot\text{MeV}$). Thus, the longitudinal emittance of the initial beam 2% leads to a 20% increase after the fragmentation, and the fragments are accepted into the secondary beam within the narrow region of the longitudinal momentum distribution. The maximal yield of the fragments is provided when the fragments are accepted in the vicinity of the maximum in the momentum distribution, corresponding to the optimal conditions for the fragment acceptance.

For now, the nuclear fragmentation at the energies $E < 100 A\cdot\text{MeV}$ is well studied, parametrizations of the fragment yields and different standard approaches are suggested for calculations of the fragmentation, giving a good description of the experimental data at higher energies, $E > 100 A\cdot\text{MeV}$, where the Q-value of the reaction is negligibly small compared to the beam energy. At the energies comparable to the Q value, the regard for the energy and momentum conservation laws is important.

For now, theoretical description of the differential and inclusive cross sections of the fragmentation at low energies, where the transferred momentum and momentum of the beam are of the same order of magnitude, is problematic. We suggest an

approach based on the Glauber model. It takes into account the energy and momentum conservation laws, and simultaneously keeps the simplicity and transparency of the Glauber model.

In this approach, it is possible to get an analytical expression for the amplitude of the process, and correct it by the factor of the phase volume thus taking into account the conservation laws.

In the present paper we apply the suggested approach for calculations of the ^{11}B fragmentation in the Be target at the energy $35A\cdot\text{MeV}$. This is the lightest nucleus where the few-proton removal leads to the production of the ^{10}Be , ^9Li , ^8He fragments. All these nuclear fragments are thoroughly experimentally studied, providing input parameters for our approach. We analyze the changes of the phase volume and the longitudinal momentum distributions with the beam energy and mass number of the fragments. We compare the momentum distributions to those obtained with the systematics widely used for calculations of the fragmentation [3], [4]. We also discuss applicability of our approach.

2 Model description

We deduce the cross section and amplitude of the scattering process within the scattering T-matrix formalism. In its terms, the differential cross section is expressed as

$$d\sigma = \frac{d\omega}{j} = |T|^2 dV^{(n)} \quad (1)$$

where T denotes the T-matrix and $dV^{(n)}$ is the phase volume of n -body system of fragments.

We suggest an approach where instead of the T-matrix we substitute the inelastic scattering amplitude multiplied by the Lorentz-invariant phase volume.

To find the amplitude we consider the fragmentation of the projectile (P) in the target (T) (See Fig. 1) assuming that the projectile is composed by fragments, which are relatively heavy core (C) and few nucleons. The initial state of the projectile is described by the wave function of the relative motion of fragments with coordinates \mathbf{r}_i . We consider the problem in the projectile rest frame. \mathbf{K} is the initial target momentum and \mathbf{K}' is that in the final state. So we define \mathbf{Q} as the target transferred

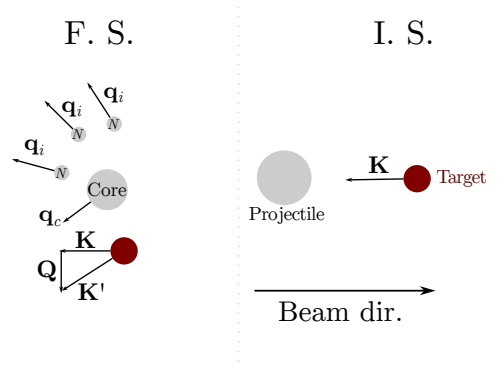


Fig. 1. Kinematical scheme of the fragmentation reaction and kinematical variables used in the model.

momentum in the projectile rest frame, \mathbf{q}_i are the projectile fragment momenta. Also we define the longitudinal l_i (with respect to \mathbf{K}) and transversal \mathbf{t}_i components of \mathbf{r}_i .

If we consider the initial wave function (WF) of the projectile as

$$\Psi_I \equiv \Psi_I(\mathbf{r}_1, \dots, \mathbf{r}_n),$$

where n is the total number of fragments, and the final state WF as

$$\Psi_F \equiv \Psi_F(\mathbf{r}_1, \dots, \mathbf{r}_n, \mathbf{q}_1, \dots, \mathbf{q}_n).$$

Within the Glauber model, neglecting the eclipse effect and re-scattering we get the amplitude of the inelastic scattering as

$$\mathcal{F}_{fi} = \sum_{j=1}^n f_j(\mathbf{Q}) \int (\Psi_F)^* e^{i\mathbf{Q}\mathbf{r}_j} \Psi_I \prod_{i=1}^n d^3\mathbf{r}_i. \quad (2)$$

Here f_j is the fragment-projectile scattering amplitude. Note, that it is assumed that \mathbf{Q} in (2) is in the plane orthogonal to the momentum \mathbf{K} , and \mathbf{q}_i should also be located in the same plane.

Our next assumption is the factorization of the WF of the initial and final states

$$\Psi_I \rightarrow \prod_{j=1}^N \Psi_{Ij}(\mathbf{r}_j)$$

and

$$\Psi_F \rightarrow \prod_{j=1}^N \Psi_{Fj}(\mathbf{r}_j, \mathbf{q}_j) \rightarrow \prod_{j=1}^N \exp[i\mathbf{r}_j\mathbf{q}_j].$$

Therefore we define functions

$$F_j(\mathbf{Q}, \mathbf{q}_1, \dots, \mathbf{q}_N) = \int d^3\mathbf{r}_j e^{i\mathbf{Q}\mathbf{r}_j} \Psi_{F_j}^*(\mathbf{r}_j, \mathbf{q}_j) \Psi_{I_j}(\mathbf{r}_j) \times \prod_{k \neq j} \int d^3\mathbf{r}_k \Psi_{F_k}^*(\mathbf{r}_k, \mathbf{q}_k) \Psi_{I_k}(\mathbf{r}_k). \quad (3)$$

After approximation of the final state WFs by the plane waves we get

$$F_j(\mathbf{Q}, \mathbf{q}_1, \dots, \mathbf{q}_N) = \int d^3\mathbf{r}_j e^{-i(\mathbf{q}_j - \mathbf{Q})\mathbf{r}_j} \Psi_{I_j}(\mathbf{r}_j) \times \prod_{k \neq j} \int d^3\mathbf{r}_k e^{-i\mathbf{q}_k\mathbf{r}_k} \Psi_{I_k}(\mathbf{r}_k) = F_j(\mathbf{q}_j - \mathbf{Q}) \prod_{k \neq j} F_k(\mathbf{q}_k). \quad (4)$$

After substitution of (4) into (2) we obtain the amplitude as

$$\mathcal{F}_{fi} = \sum_{j=1}^N f_j(\mathbf{Q}) F_j(\mathbf{q}_j - \mathbf{Q}) \prod_{k \neq j} F_k(\mathbf{q}_k).$$

We will show that $f_C \gg f_N$ so we can leave only one term in the expression.

Thus, finally, the amplitude of the inelastic scattering takes the form

$$\mathcal{F}_{fi} \approx f_c(\mathbf{Q}) F_C(\mathbf{q}_C - \mathbf{Q}) \prod_k F_N(\mathbf{q}_k), \quad (5)$$

Note here that $F_C(\mathbf{q}_C)$ is the form factor determined by the nucleus size. Thus, the inelastic scattering amplitude is defined by the elastic scattering amplitude of the core $f_C(\mathbf{Q})$. The interaction with nucleons enters the form factors $F_N(\mathbf{q}_k)$. The obtaining of this expression is given in [1].

We approximate the functions F_C and F_N by the oscillator function in the momentum space as

$$F_j(q) = \sqrt[4]{\frac{32}{27} \pi \langle r_j \rangle^6} e^{-\frac{4}{3} q^2 \langle r_j \rangle^2}; \quad (6)$$

where $\langle r_j \rangle$ is root mean squared radius (RMS) of the fragment WF.

The elastic scattering amplitude $f_C(\mathbf{Q})$ is calculated in the Glauber model using the corresponding core -target profile function S_C as

$$f_C(\mathbf{Q}) = \langle \Psi_F | S_C | \Psi_I \rangle$$

where the profile function is obtained using the optical model potential

$$S_C(b) = \exp \left[-\frac{i}{\hbar v} \int_{-\infty}^{\infty} dz V_{CT}(\sqrt{b^2 + z^2}) \right], \quad (7)$$

where $V_C(r)$ is the optical potential describing the core-target interaction. b is the impact parameter of the center of mass of the core (see, for example, [5, 6] and references therein). v is the beam velocity, and z is the coordinate along the beam axis.

There are a lot of parametrizations of the optical model parameters available in the literature. In our case, when we develop the approach for a very wide projectile energy range, we use the standard parametrization of the nucleon-nucleon interaction potential with the parameters from [7, 8], which is valid for the incident energy range from 10 to 2000 A-MeV.

2.1 Folding Model of the Optical Potential

The nucleon-nucleon potential describes the interaction of each nucleon composing the nucleus with each nucleon of the target. To calculate the optical potential of the core-target interaction we find the folding [9] of the potential with the nucleon densities.

The core-target interaction potential in the folding model can be expressed as follows:

$$V_C(\mathbf{r}) = \int A_C \rho_C(\mathbf{r}') \overline{V_{CT}}(|\mathbf{r} - \mathbf{r}'|) d\mathbf{r}'. \quad (8)$$

where

$$\overline{V_{CT}}(|\mathbf{r} - \mathbf{r}'|) = -\frac{i}{2} \hbar v A_T \rho_T(|\mathbf{r} - \mathbf{r}'|) \overline{\sigma_{NN}} \quad (9)$$

The density distribution of the interacting nuclear systems is approximated by a Gaussian distribution [10]:

$$\rho(x) = \rho_0 \exp(-\alpha x^2), \quad (10)$$

where $\alpha = \left[\frac{2}{3} \langle r^2 \rangle \right]^{-1}$ is the density distribution parameter related to RMS of the nucleus $\langle r^2 \rangle^{1/2}$, and $\rho(x)$ is normalized to unity. $\overline{\sigma_{NN}}$ is the nucleon-nucleon cross-section averaged over the number of neutrons and protons involved in the interaction (for more details, see [7], [8]).

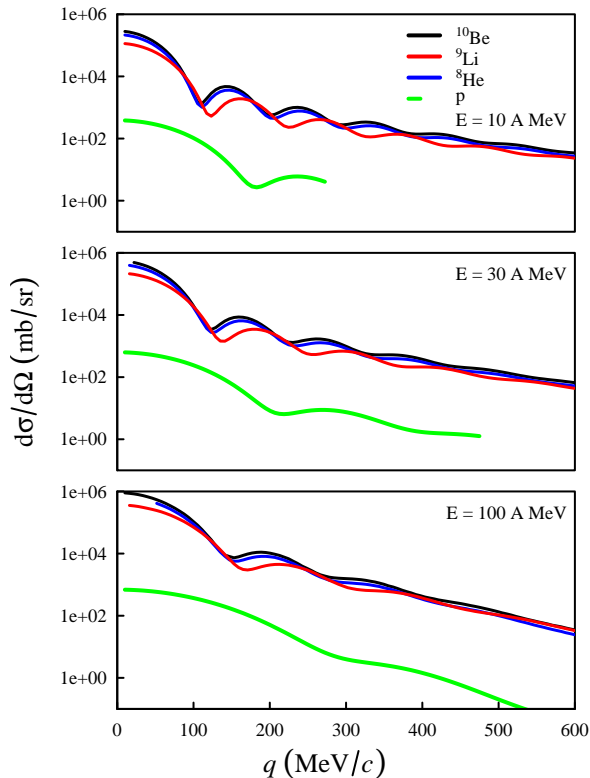


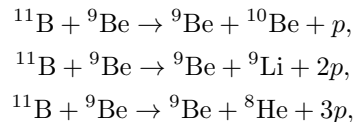
Fig. 2. Differential elastic scattering as a function of the transferred momenta q for scattering of protons and heavy ions (^{10}Be , ^9Li , and ^8He) on the ^9Be target for different projectile energies. (see the legends on the panels.)

Table 1. The RMS radii of heavy fragment used in the calculations. $\langle r_c \rangle$ is the default value; $\min\langle r_c \rangle$ is the radii for case of “more central” reaction; $\max\langle r_c \rangle$ is the radii for case of “more peripheral” reaction. (all the values are given in fm,)

Fragment	$\langle r_c \rangle$	$\min\langle r_c \rangle$	$\max\langle r_c \rangle$
^{10}Be	0.2426160	0.1213080	0.4852321
^9Li	0.4852321	0.2426160	0.9704641
^8He	0.7278481	0.3639241	1.4556962

3 Results and discussion

As mentioned above, we consider three reactions (for different beam energies)



which “illustrate” the path towards the neutron dripline.

In our model, we consider the projectile nucleus ^{11}B as a system of pre-formed heavy cluster and valence protons. The structure of ^{11}B is described by the corresponding form factor $F_C(\mathbf{q}_C)$ in (6) determined by the RMS distance of the core inside ^{11}B . In our calculations, we used the proton RMS distance $\langle r_p \rangle = 2.43$ (fm) taken in accordance with the standard systematics [11]. As the first approach one can obtain $\langle r_C \rangle$ supposing the core to be a particle. The values of $\langle r_C \rangle$ are presented in the Table 1. Since the core WF inside ^{11}B may be more complicated, we vary $\langle r_C \rangle$ in a wide range (see also the Table 1) to demonstrate sensitivity of our model to this parameter.

For the calculations of the reaction rate (5) the Monte Carlo method is used.

The Figs. 3 and 4 show the correlation plots for the target transferred momentum (Q) vs. projection of the core momentum in the projectile rest frame where the z axis coincides with the beam direction, and similar dependence of the two projections of the core momentum in the projectile rest frame (q_{cx} and q_{cz}).

The kinematical loci of the fragments can be easily recognized in Figs. 3 and 4. Considering these

graphs, few moments should be pointed out which are as follows: (i) for the low beam energies, 10 and 30 MeV, the variables Q and q_{cz} are strongly correlated; this correlation becomes weaker with increase in the number of fragments; (ii) the loci of q_{cz} are asymmetric relative to the beam speed point, so there is a tendency of “slowing down” of the fragment at low energies related with the reaction kinematics.

In the calculations of the elastic scattering, we expected that the dominant part of the elastic scattering cross section corresponds to the transferred momentum lower than that of the first diffraction minimum (See Fig. 2). Note, that kinematic locus in this case contains the non-zeroth transferred momentum Q since the part of the beam energy is spent for the nucleon knock-out. Therefore, the case of the Serber model [12], which is valid for the limit $Q = 0$ MeV/c, is not realized due to the kinematical locus. In this case the fragments are slower than the beam nuclei.

This result shows necessity of the momentum and energy conservation laws at low energies. From this viewpoint, the models of the sudden removal with $Q = 0$, such as the Serber model and the traditional eikonal approximation of the Glauber model, give only qualitative description, and don't reproduce the position of the momentum distributions, while their widths are close to those obtained in our approach.

Sensitivity of our calculation to the $\langle r_C \rangle$ parameter is illustrated by Figs. 5 and 6. The variation of the results of the calculations with this parameter can be explained as follows: in the case of the small values of $\langle r_C \rangle$ for the particular reaction channel, the central collisions dominates, while the large values of $\langle r_C \rangle$ the peripheral process becomes essential. To demonstrate these effects we performed the calculations with different values of $\langle r_C \rangle$, the minimal, default, and maximal ones presented in the Table 1.

Figure 5 shows the changes of the mode (peak position), standard variation, and skewness of the q_{cz} distribution with the $\langle r_C \rangle$ value. The qualitative behavior of the q_{cz} distribution remains the same. For the peripheral case, one can see “speed-up” of the fragment, (for the high energy q_{cz} is faster than the beam velocity point) and narrowing of the q_{cz} distribution. For the central case, the q_{cz} distribution becomes wider and more asymmetric.

Finally in Figure 6 we compare the calculated width of the longitudinal momentum distributions of the fragment with the widely used Goldhaber model [3]. For the high beam energy $E_b = 100 A$ MeV and $E_b = 30 A$ MeV our results are in the reasonable agreement with [3]. For the low beam energy $E_b = 10 A$ MeV the fragment mass number dependence of the widths of the longitudinal momentum distributions in our calculations qualitatively differs from that obtained in [3].

4 Summary

One of the most traditional ways of the exotic (neutron or proton-rich) nuclei production is the fragmentation of the beam nuclei. To provide the effective production of a certain isotope the preliminary calculations are needed. At the energies $E < 100 A$ -MeV, traditional sudden removal approaches are not precise.

We suggest the approach based on the Glauber model modified for regard for the energy and momentum conservation laws. For calculations of the amplitude of the fragmentation reaction, the Lorentz-invariant phase space is introduced. The analytical solution exists for the case of the elastic scattering. The parameters of the approach, such as rms radii of a nucleus and the related rms distance between core and valence nucleons in the exotic nuclei, the optical model parameters, etc., are well known, and can be found in literature on the experimental data and parametrizations.

With the example of the ^{11}B fragmentation we have calculated the longitudinal momentum distributions of the ^{10}Be , ^9Li , and ^8He fragments. The relation between the longitudinal momentum distribution and number of removed nucleons is studied, as well as the fragment mass and beam energy dependence are analyzed. It is found that the heavier the target, the better the precision of the approach. We also see, that for the energies below 100 MeV the fragments are slower than the beam nuclei, that is defined by the kinematic locus, while for the high energies ($>100 A$ MeV) the fragment may appear to have both higher or lower speed depending on geometry of the reaction. In particular, more peripheral reactions lead to faster fragments, and less peripheral (central) reactions provide the slower fragments with respect to the beam velocity.

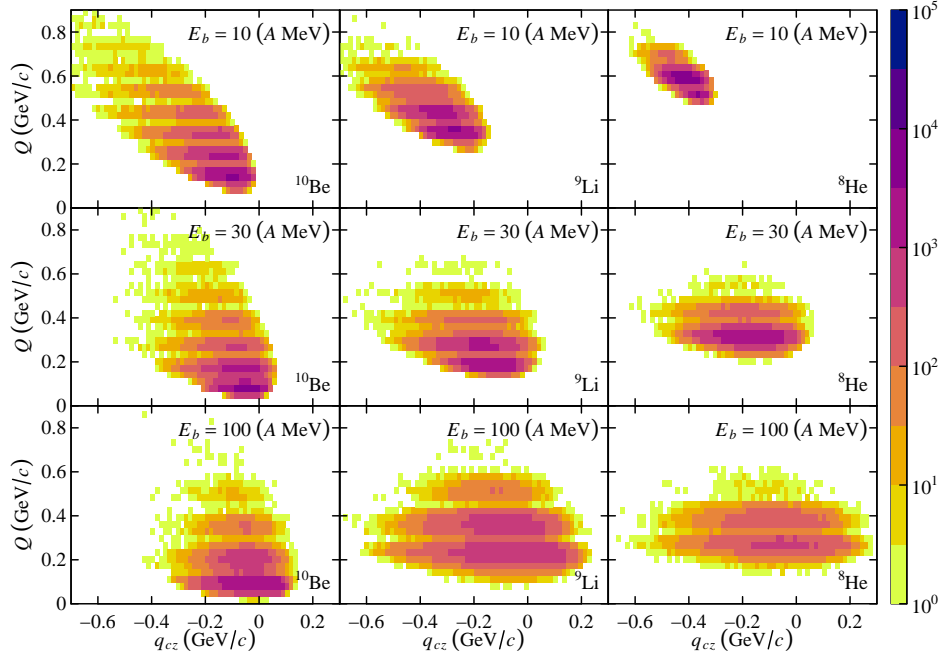


Fig. 3. Correlation of the transferred momentum of target Q and longitudinal part q_{cz} of the core momentum in the projectile rest frame for different fragments (shown in bottom right panel corner) and different ^{11}B beam energies (shown in top right panel corner).

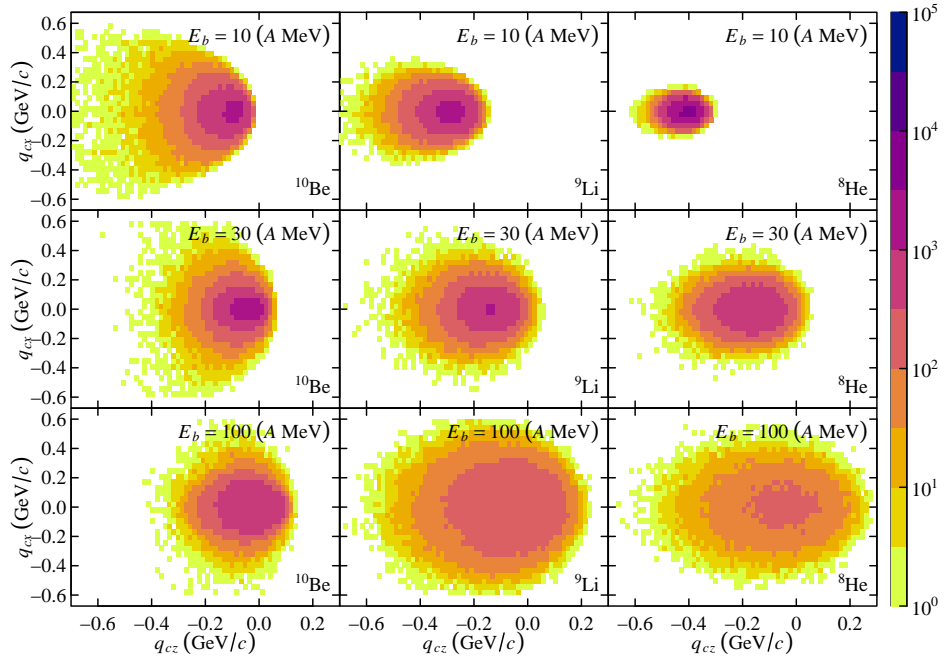


Fig. 4. Correlation of the transversal q_{cx} and longitudinal q_{cz} parts of the core momentum in the projectile rest frame. The layout is the same as in Figure 3.

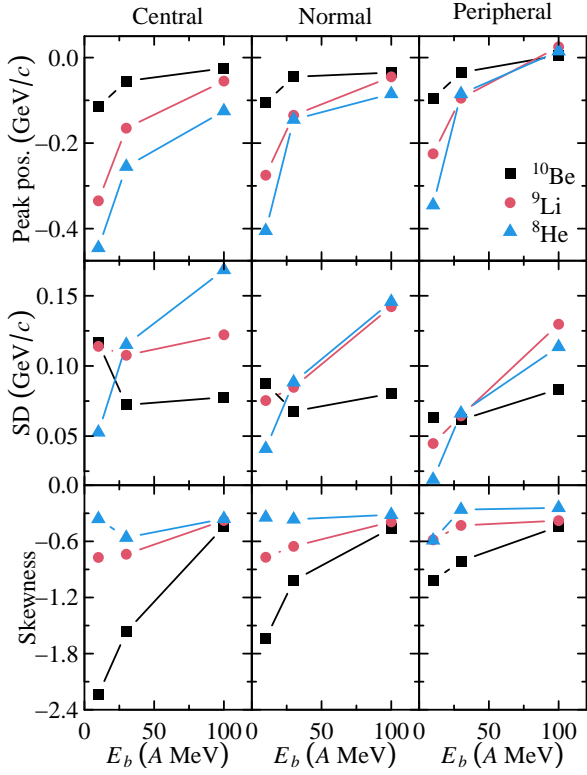


Fig. 5. The mode (peak position), standard variation (SD), and skewness for different values of $\langle r_C \rangle$ (see the Table 1).

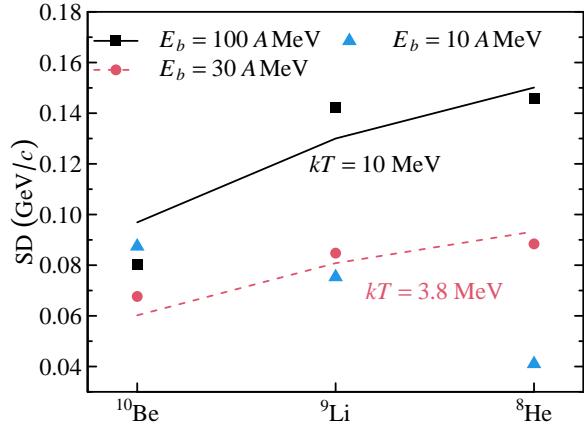


Fig. 6. Comparison of standard deviation (SD) of q_{cz} obtained in our calculations (points) and that obtained in the model [3] (lines). The values of kT (see [3]) for the beam energy $E_b = 100$ A MeV and $E_b = 30$ A MeV are presented in the panels.

The regard for the energy and momentum conservation laws leads to essential changes in the shape of the longitudinal momentum distributions, showing asymmetry, where the low momentum tail of the distribution is formed due to the large transferred momentum. Thus, compared to the Glauber model our approach describes the fragmentation in a wider range of momentum transfer. The Glauber provides a good description within the momentum transfer 100-150 MeV/c. The applicability of our approach for the momentum transfer beyond the first diffraction minima needs more detailed studies. In the present paper we show, that the transfer on nucleons can proceed with the momentum transfer essentially exceeding that corresponding to the first diffraction minimum. The approach allows to reproduce the wide momentum distributions in this case.

The comparison with calculations within other models and parametrizations shows that at the energies less than 100 A-MeV the kinematical loci and energy-momentum conservation laws should necessarily be taken into account while planning the experiment and finding the optimal conditions for the fragment production.

References

- [1] R. J. Glauber. High-energy collision theory. *Geometrical pictures in hadronic collisions*, pages 83–182, 1987.
- [2] O. Tarasov. Analysis of momentum distributions of projectile fragmentation products. *Nuclear Physics A*, 734:536–540, 2004.
- [3] Alfred S. Goldhaber. Statistical models of fragmentation processes. *Physics Letters B*, 53(4):306–308, 1974.
- [4] D. J. Morrissey. Systematics of momentum distributions from reactions with relativistic ions. *Physical Review C*, 39(2):460, 1989.
- [5] K. Hencken, G. Bertsch, and H. Esbensen. Breakup reactions of the halo nuclei be 11 and b 8. *Physical Review C*, 54(6):3043, 1996.
- [6] Yu. L. Parfenova, M. V. Zhukov, and J. S. Vaagen. Breakup of 11 be and 15 c on light targets including core excitations. *Physical Review C*, 62(4):044602, 2000.
- [7] S. K. Charagi and S. K. Gupta. Coulomb-modified glauber model description of heavy-

- ion reaction cross sections. *Physical Review C*, 41(4):1610, 1990.
- [8] L Ray. Proton-nucleus total cross sections in the intermediate energy range. *Physical Review C*, 20(5):1857, 1979.
- [9] R. L. Varner, W. J. Thompson, T. L. McAbee, E. J. Ludwig, and T. B. Clegg. A global nucleon optical model potential. *Physics Reports*, 201:57–119, 1991.
- [10] Yu. L. Parfenova and M. V. Zhukov. $8b$ breakup on $12c$ at intermediate energies and the three-body structure of $8b$. *Physical Review C*, 66(6):064607, 2002.
- [11] A. István and K Marinova. Table of experimental nuclear ground state charge radii: An update. *Atomic Data and Nuclear Data Tables*, 99(1):69–95, 2013.
- [12] R. Serber. Theory of scattering with large momentum transfer. *Physical Review Letters*, 10(8):357, 1963.